

The collimated outflows of the planetary nebula Hu 1-2: proper motion and radial velocity measurements^{*}

L.F. Miranda^{1,2†}, M. Blanco^{3†}, M.A. Guerrero^{3†}, A. Riera^{4†}

¹ *Departamento de Física Aplicada, Facultad de Ciencias, Campus Lagoas-Marcosende s/n, Universidade de Vigo, E-36310 Vigo, Spain (present address)*

² *Consejo Superior de Investigaciones Científicas, C/ Serrano 117, E-28006 Madrid, Spain*

³ *Instituto de Astrofísica de Andalucía – CSIC, C/ Glorieta de la Astronomía s/n, E-18008 Granada, Spain*

⁴ *Departament de Física i Enginyeria Nuclear, EUETIB, Universitat Politècnica de Catalunya, Compte d’Urgell 187, E-08036 Barcelona, Spain*

Accepted. Received; in original form

ABSTRACT

Hu 1-2 is a planetary nebula that contains an isolated knot located northwestern of the main nebula, which could be related to a collimated outflow. We present a subsarc-second $H\alpha + [N\ II]$ image and a high-resolution, long-slit spectrum of Hu 1-2 that allow us to identify the southeastern counterpart of the northwestern knot and to establish their high velocity ($> 340\text{ km s}^{-1}$), collimated bipolar outflow nature. The detection of the northwestern knot in POSS red plates allows us to carry out a proper motion analysis by combining three POSS red plates and two narrow-band $H\alpha + [N\ II]$ CCD images, with a time baseline of $\simeq 57$ yr. A proper motion of $20 \pm 6\text{ mas yr}^{-1}$ along position angle $312^\circ \pm 15^\circ$, and a dynamical age of $1375 \pm_{320}^{590}$ yr are obtained for the bipolar outflow. The measured proper motion and the spatio-kinematical properties of the bipolar outflow yield a lower limit of 2.7 kpc for the distance to Hu 1-2.

Key words: planetary nebulae: individual: Hu 1-2 – ISM: jets and outflows – ISM: kinematics and dynamics

1 INTRODUCTION

Planetary nebulae (PNe) represent the final evolutionary stages of low- and intermediate-mass stars. They are formed when the envelope ejected during the previous Asymptotic Giant Branch phase is ionized by the hot central star. In the last years the presence of collimated bipolar outflows in PNe has been widely recognized. These outflows probably play a crucial role in the shaping and dynamical evolution of PNe (Sahai & Trauger 1998). Therefore, the knowledge of their dynamical properties is critical to understand how PNe form. The kinematics of the outflows has been studied by means of high-resolution spectroscopy that permits to obtain the radial component of the velocity (e.g., Miranda et al. 1999, 2001; Guerrero et al. 2000). The measurement of the tangential component, i.e., the proper motion of collimated outflows, is restricted to a very few cases and it has

been obtained mostly from *HST* observations (NGC 7009: Fernández et al. 2004; He 2-90: Sahai et al. 2002; Hen 3-1475: Borkowski & Harrington 2001; Riera et al. 2003) or *VLA* radio continuum data (NGC 7009: Rodríguez & Gómez 2007) with the noticeable exceptions of the works by Liller (1965) and Meaburn (1997) who used photographic material to measure proper motions of the collimated outflows in NGC 7009 and KjPn 8, respectively. The measurement of proper motions is important because it allows us to obtain the distances to the PN, if the expansion velocity of the outflows is known (e.g., Meaburn 1997), or the expansion velocity vector, if the distance is known (e.g., Fernández et al. 2007). Therefore, further measurements of proper motions of collimated outflows in PNe are highly desirable.

Collimated outflows may exist in the PN Hu 1-2 (PN G086.5–08.8) that has been classified as elliptical with ansae (Manchado et al. 1996). The kinematics of the inner nebular regions ($\simeq 10''$) of Hu 1-2 was analyzed by Sabbadin et al. (1983, 1987). These authors identified a toroid and bipolar lobes but a reconstruction of the spatio-kinematical structure was not possible because of the peculiar velocity field. In addition, one single knot can be hinted in the images by Manchado et al. (1996) northwestwards and well outside the main nebula, while a possible southeastern counter-

^{*} Based on observations made with the Nordic Optical Telescope (NOT) which is operated jointly by Denmark, Finland, Iceland, Norway, and Sweden on the island of La Palma in the Spanish Observatorio del Roque de los Muchachos of the Instituto de Astrofísica de Canarias (IAC).

[†] E-mail: lfm@iaa.es (LFM); blanco@iaa.es (MB); mar@iaa.es (MAR); angles.riera@upc.edu (AR)

part is superimposed by a field star. Remarkably, the north-western knot can be identified in POSS red plates of the Digitized Sky Surveys. In this respect, Hu 1-2 constitutes a rare case (together with NGC 7009 and KJpN 8) because knots/collimated outflows in PNe usually are weak and/or located close to the much brighter main nebula, which do not favor their detection in POSS plates. Moreover, the $H\alpha$ and $[N II]$ emission lines are by far the dominant emissions from knots/collimated outflows in PNe in the optical (e.g., Balick 1993, 1994), as it is the case of the northwestern knot of Hu 1-2. In consequence, the emission from the northwestern knot of Hu 1-2 detected in the POSS red plates can be attributed to these two emission lines. Therefore, Hu 1-2 offers an excellent opportunity to attempt a proper motion analysis of knots/collimated outflows in PNe by combining POSS red plates with modern $H\alpha+[N II]$ imagery.

In this paper we present a new $H\alpha+[N II]$ image of Hu 1-2 obtained under subsecond conditions, and a high resolution, long-slit spectrum that allow us to identify the southeastern counterpart of the northwestern knot and to establish that these two knots constitute a high velocity, collimated bipolar outflow. In addition, we carry out an analysis of five images obtained at different epochs, including three images from the POSS, to measure the proper motion of the northwestern knot and to constrain the distance to Hu 1-2.

2 OBSERVATIONS

2.1 Direct images

The five images of Hu 1-2 analyzed in this paper are the following:

- Epoch 1: 1951.51. Image from the POSSI-E, plate 08HM, obtained on 1951 June 5 with the Palomar Schmidt telescope on a 103aE plate with a plexi filter. The exposure time was 50 minutes. It is digitized with a plate scale of $1''.70 \text{ pixel}^{-1}$ and its spatial resolution (FWHM of field stars) is $\simeq 3''.5$.

- Epoch 2: 1953.68. Image from the POSSI-E, plate 089E, obtained on 1953 September 5 with the Palomar Schmidt telescope, on a 103aE plate with a plexi filter. The exposure time was 45 minutes. The plate scale is $1''.70 \text{ pixel}^{-1}$ and its spatial resolution is $\simeq 3''.0$.

- Epoch 3: 1987.56. Image from the POSSII-F, plate A114, obtained on 1987 July 26 with the Oschin Smith Telescope on a IIIaF plate with a RG610 filter. The exposure time was 75 minutes. The plate scale is $1''.01 \text{ pixel}^{-1}$ and its spatial resolution is $\simeq 3''.0$.

- Epoch 4: 1994.54. Image from the IAC Morphological Catalog of Northern Galactic PNe (Manchado et al. 1996) obtained on 1994 July 24 with the IAC80 telescope (Observatorio del Teide, Tenerife), on a $1k \times 1k$ CCD Thomson with an $H\alpha+[N II]$ filter (FWHM $\simeq 50 \text{ \AA}$). The exposure time was 3600 seconds. The plate scale is $0''.435 \text{ pixel}^{-1}$ and its spatial resolution is $\simeq 2''.2$.

- Epoch 5: 2008.67. $H\alpha$ and $[N II]$ images obtained on 2004 July with ALFOSC¹ at the Nordic Optical Telescope (NOT,

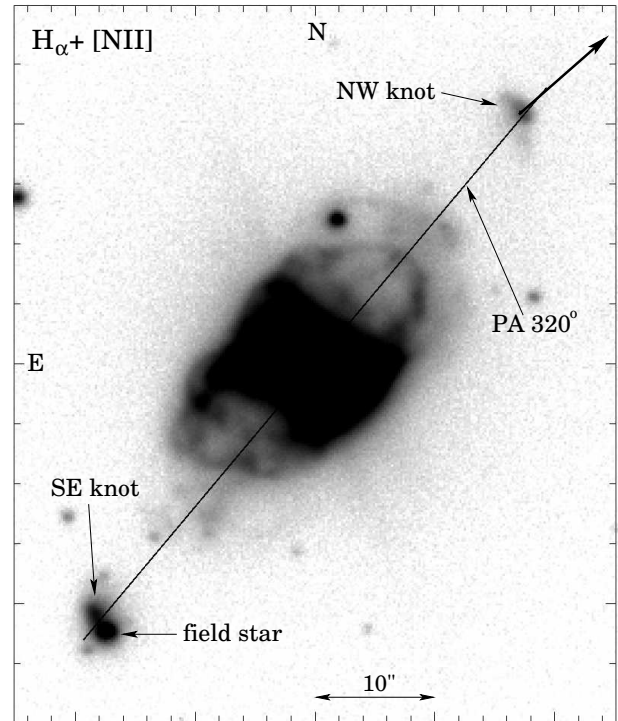


Figure 1. Grey-scale reproduction of the 2008.67 $H\alpha+[N II]$ image of Hu 1-2. The grey levels are logarithmic. The NW and SE knots are indicated as well as a field star partially superimposed on the SE knot. The slit position used for high resolution spectroscopy is drawn and labeled by its position angle (slit width not to scale). The arrow at the NW knot indicates the shift ($10''$) and its direction (PA 312°) expected in 500 yr, according to the proper motion deduced for this knot (see text). North is up, east to the left, and the scale is indicated.

Roque de los Muchachos, La Palma), on a $2k \times 2k$ EEV CCD. We use the IAC narrow-band $H\alpha$ (FWHM $\simeq 8 \text{ \AA}$) and $[N II]$ (FWHM $\simeq 9 \text{ \AA}$) filters. The exposure time was 900 s for each filter. The plate scale is $0''.19 \text{ pixel}^{-1}$ and its spatial resolution is $0''.85$. The individual $H\alpha$ and $[N II]$ frames were co-added to produce the $H\alpha+[N II]$ image of epoch 5 shown in Figure 1.

The images were registered with routines within the MIDAS package, using the 2008.67 image as reference, by means of 11 faint field stars that do not show noticeable proper motions in the $\simeq 57$ yr time baseline. After the registering process, the positions of the 11 fiducial stars (defined by their centroid) in the 2008.67 epoch are within $< 0''.1$ their positions in the 1951.51 and 1953.68 epochs and within $< 0''.06$ their positions in the 1987.56 and 1994.54 epochs. The resulting intrinsic error in the proper motion between the different epochs ($< \pm 0.9 \text{ mas yr}^{-1}$) is negligible and does not affect the measurement of nebular proper motions.

¹ ALFOSC (Andalucía Faint Object Spectrograph and Camera) is provided by the Instituto de Astrofísica de Andalucía (IAA)

under a joint agreement with the University of Copenhagen and NOTSA.

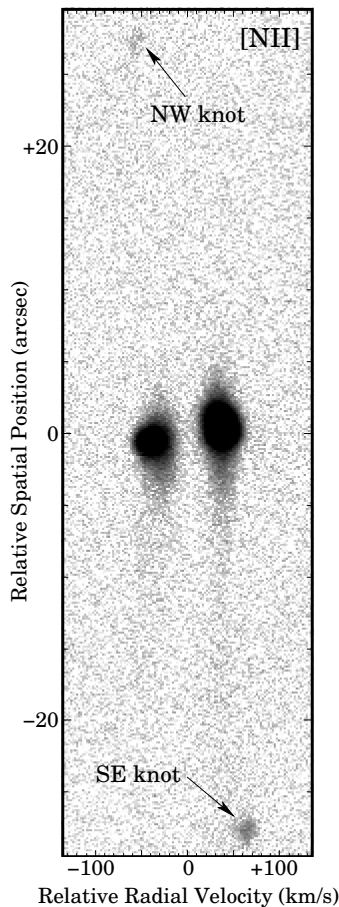


Figure 2. Grey-scale position-velocity map of the $[\text{N II}]\lambda 6583$ emission line along PA 320° (see Fig. 1). Grey levels are logarithmic. Emission features from the NW and SE knots are indicated. The origin (0,0) corresponds to the spatial and radial velocity centroid of the relatively bright emission features from the inner nebular regions.

2.2 High resolution spectroscopy

A high resolution long-slit spectrum of Hu 1-2 was obtained with IACUB² at the Nordic Optical Telescope (NOT) on Roque de los Muchachos Observatory (La Palma) on 2004 June. We used a $1\text{k}\times 1\text{k}$ Thompson CCD and a narrow-band filter to isolate the $\text{H}\alpha$ and $[\text{N II}]\lambda\lambda 6548, 6583$ emission lines. The slit ($0''.65$ wide) was oriented at position angle (PA) 320° , the orientation of the knots of Hu 1-2 (see below). The orientation of the slit is also shown in Fig. 1. Exposure time was 900 s. The spectral resolution (FWHM) is 8 km s^{-1} and the seeing was $\simeq 1''$. The spectrum was reduced using standard procedures for long-slit spectroscopy within the IRAF package. Figure 2 presents a position-velocity map of the $[\text{N II}]\lambda 6583$ emission line obtained from this spectrum.

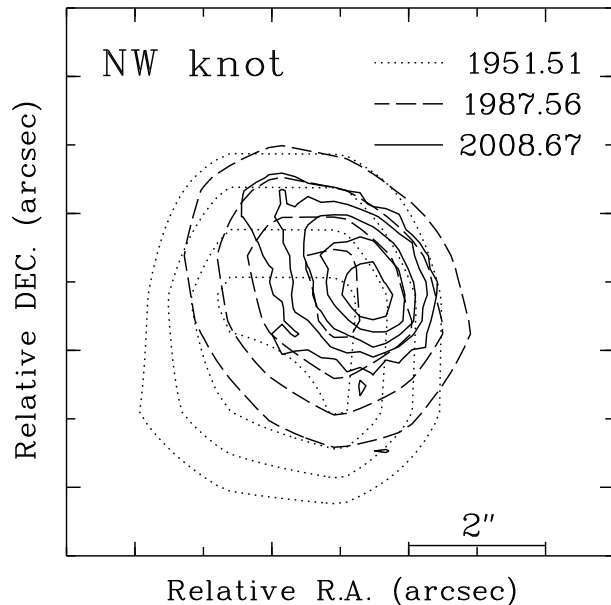


Figure 3. Intensity contour plots of the NW knot derived from the images of the 1951.51, 1987.56 and 2008.67 epochs after registering. The contours are arbitrary and have been chosen to highlight the regions of the knot around the intensity peak. North is up, east to the left.

3 RESULTS AND DISCUSSION

The image in Fig. 1 shows Hu 1-2 consisting of an elliptical/bipolar main shell of $\simeq 14''\times 24''$ in size and oriented at PA $\simeq 320^\circ$, and reveals several outer structures around the polar regions of the main shell (see Miranda et al. 2011 for a description of the morphological components in Hu 1-2). The northwestern knot hinted by Machado et al. (1996) is clearly detected in the 2008.67 image. The southeastern counterpart is identified in this image for the first time owing its subarcsecond spatial resolution that permits to separate the knot from a very close field star. We will refer to them as the NW and SE knots. They present bow-shock-like morphology with a central emission peak and extended wings, are located at $27''.5$ from the central star of Hu 1-2 (Heap et al. 1990; Miranda et al. 2011), and oriented at PA 320° that coincides with the orientation of the main nebular axis. The SE knot is brighter than the NW one.

Emission features from the bipolar knots are detected in the long-slit spectrum (Fig. 2) with radial velocities of $\pm 60\text{ km s}^{-1}$ (NW knot blueshifted, SE knot redshifted). The inclination angle of the knots is unknown. From an analysis of high-resolution, long-slit $\text{H}\alpha$ spectra at several PAs, Miranda et al. (2011) obtained an upper limit of 10° with respect to the plane of the sky for the inclination of the main nebular axis of Hu 1-2 (see also Miranda et al. 2012 in preparation). If the knots moved along the main nebular axis, as suggested by the coincidence of the orientations, their expansion velocity would be $> 340\text{ km s}^{-1}$. It should be noted that a more accurate value for the expansion velocity cannot be obtained mainly because of the very small inclination angle of the object (see below). In any case, these results conclusively demonstrate that the NW and SE knots constitute a high velocity, collimated bipolar outflow. Moreover, the morphological and kinematical properties point out

² The IACUB uncrossed echelle spectrograph was built in a collaboration between the IAC and the Queen's University of Belfast

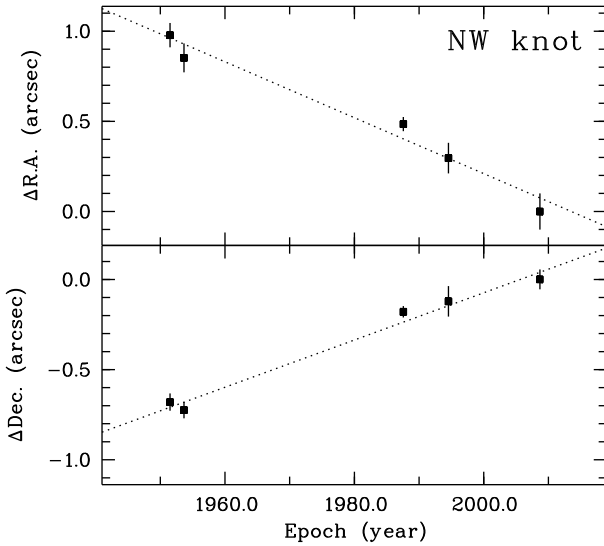


Figure 4. Position of the centroid of the NW knot versus time, relative to the position in the 2008.67 epoch. Error bars are 3σ values. The dotted lines represent least-squares fits to the data.

that the NW and SE knots represent the working surfaces of high-velocity bullets. We also note that the expansion velocity of these knots is high for collimated outflows in PNe (see Guerrero et al. 2002) and only in a few cases expansion velocities $> 300 \text{ km s}^{-1}$ are observed (e.g., Riera et al. 2003; Guerrero & Miranda 2011)

Figure 3 shows intensity contour plots of the NW knot derived from the images of the 1951.51, 1987.56 and 2008.67 epochs after registering. In spite of the different spatial resolution in the images, a preliminary inspection of Fig. 3 shows that the intensity peak of NW knot has shifted towards the northwest in the last ≈ 57 years. This is corroborated by the 1953.68 and 1994.54 images (not shown in Fig. 3 for clarity). A quantitative measurement of the position of the NW knot (defined by its centroid) was obtained by fitting a two dimensional Gaussian line profile to the intensity distribution of the knot in each epoch. Figure 4 presents the relative α and δ positions of the NW knot as a function of time (epoch). Least-squares fits to the data in Fig. 4 yield a proper motion (μ) $\mu_\alpha = -15.5 \pm 5.0 \text{ mas yr}^{-1}$ and $\mu_\delta = +13.1 \pm 3.1 \text{ mas yr}^{-1}$. By combining these values and their errors, we obtain a proper motion for the NW knot $\mu = 20 \pm 6 \text{ mas yr}^{-1}$ along $\text{PA} = 312^\circ \pm 15^\circ$. The direction of the proper motion vector agrees quite well with the orientation of the main nebular axis and bipolar knots, strengthening the idea that the collimated outflow move along that axis. Assuming ballistic ejection and origin at the central star, we obtain a dynamical age of $1375_{-320}^{+590} \text{ yr}$ for the NW knot.

A similar proper motion analysis cannot be carried out for the SE knot as it has been only detected in the 2008.67 image. However, the spatio-kinematical properties (morphology, distance to the central star and radial velocity) of the SE knot are virtually identical to these of the NW knot. Therefore, it can be inferred that other properties (proper motion vector, origin, age) are also identical in both knots, too.

From the expansion velocity of 340 km s^{-1} and the proper motion of $20 \pm 6 \text{ mas yr}^{-1}$ of the knots, we obtain

a distance of $3.5_{-0.8}^{+1.5} \text{ kpc}$ to Hu 1-2, with a lower limit of 2.7 kpc giving the uncertainty in μ and that 340 km s^{-1} is a lower limit to the expansion velocity. As already mentioned, the very small inclination angle (from the sky) of the NW and SE knots represents a problem to obtain a more accurate value for the expansion velocity and, hence, for the distance. In Hu 1-2, the assumption that the NW and SE knots move along the main nebular axis is strongly supported by the coincidence of their orientations and the direction of the proper motion. As for the inclination of the main nebular axis, Miranda et al. (2011) obtain an upper limit of 10° from the sky, being inclination angles of, say, 2° , 5° or 7° also compatible with the observed spatio-kinematical properties of the main shell. An uncertainty of a few degrees in the inclination angle is extremely critical in the determination of the expansion velocity for inclination angles $< 10^\circ$. For instance, if the NW and SE knots move at 5° from the sky (only 5° less than the upper limit of 10°), their expansion velocity is 688 km s^{-1} and the lower limit for the distance results to be 5.6 kpc , a factor > 2 larger than the value deduced for an angle of 10° . Unless the expansion velocity (or inclination angle) of the NW and SE knots can be very much constrained by some method, the proper motion method will provide a lower limit for the distance only.

It is interesting to compare the lower limit of 2.7 kpc with other distance estimates to Hu 1-2. Statistical distances range between 1.3 kpc (Amnuel et al. 1984) and 5.6 kpc (Cahn 1976; see also Acker et al. 1992, Phillips 2004, and Stanghellini & Haywood 2010). Pottasch (1983) and Sabbadin (1986) obtained an individual distance of $1.5\text{--}1.6 \text{ kpc}$ by the extinction method. Hajian & Terzian (1996) set a lower limit of 1.2 kpc from the non detection of angular expansion in VLA 6 cm radio continuum data at two epochs. The lower limit of 2.7 kpc rules out a large fraction of the statistical distances. For statistical distances $> 2.7 \text{ kpc}$ (e.g., Cahn 1976; Stanghellini & Haywood 2010) the uncertainty in the expansion velocity does not allow us to drawn firm conclusions from possible coincidences. In general, this result points out that statistical distances based on assumptions about nebular properties should be used with caution when analyzing individual PNe (see Frew 2008 and Tafuya et al. 2011). Furthermore, the extinction distance is also excluded, most probably because Hu 1-2, at a galactic latitude of ≈ -8.8 , is located outside the interstellar reddening layer and the extinction method provides a too small distance (see Phillips 2006).

As shown above, proper motions of collimated outflows in PNe, if detected in POSS red plates, can be obtained by comparing these plates with recent $\text{H}\alpha + [\text{N II}]$ CCD images. This is due to the very peculiar optical spectrum of collimated outflows in PNe, which is entirely dominated by $\text{H}\alpha$ and $[\text{N II}]$ emission lines and excludes a noticeable contribution from other lines in the emission detected in the POSS red plates. As for now, collimated outflows in POSS red plates have been identify in NGC 7009, KJPN 8 and Hu 1-2 (see above) but a careful inspection of these plates is desirable to identify more cases and to attempt a measurement of their proper motion. These, in conjunction with spatio-kinematical models of the collimated outflows and/or nebular shell, may provide a powerful method to obtain (or to constrain) distances to PNe. This procedure is not restricted to collimated outflows only but can also be applied

to other high velocity features (knots, filaments) in PNe if their emission in the red spectral range is dominated by the $H\alpha$ and $[N\text{II}]$ lines. In this respect it is worth noting that Meaburn et al. (2008) used an 1956 SAAO red plate and a 2007 $H\alpha+[N\text{II}]$ CCD image to successfully measure the proper motion of a large number of knots in the western lobe of NGC 6302 and to obtain its distance. While a shortcoming of the POSS red plates is their low spatial resolution (e.g., the case of the SE knot), clear advantages of these plates are the large time baseline (> 50 yr) and the possibility of using more than two epochs (including POSSI and POSSII) to determine the proper motions.

4 CONCLUSIONS

We have presented a subarcsecond $H\alpha+[N\text{II}]$ image and a high resolution long-slit spectrum of Hu 1-2 covering its bipolar knots. In addition, we have analyzed five images of Hu 1-2 with a time baseline of $\simeq 57$ yr, including three POSS red plates in which one of the bipolar knots can be identified, to measure its proper motion and to constrain the distance to the nebula. The main conclusions of this paper are:

- The subarcsecond image allows us to identify the two bipolar knots of the pair, while in previous images only one of them is clearly detected. The knots present bow-shock-like morphology, are located at $27''.5$ from the central star and oriented at PA 320° that coincides with the orientation of the main nebular axis.
- The radial velocity of the knots is ± 60 km s^{-1} . If the knots moved along the main nebular axis (tilted $< 10^\circ$ with respect to the plane of the sky), their expansion velocity would be > 340 km s^{-1} . Therefore, morphology and kinematics demonstrate that these knots constitute a true high velocity, collimated bipolar outflow and, most probably, represent bow-shocks associated to high velocity bullets.
- A proper motion of 20 ± 6 mas yr^{-1} along PA $312^\circ \pm 15^\circ$ is obtained for the bipolar knots. The corresponding dynamical age is 1375^{+590}_{-320} yr.
- A lower limit of 2.7 kpc for the distance to Hu 1-2 is required to make compatible the measured proper motion with the spatio-kinematical properties of the bipolar outflow. This lower limit rules out a large fraction of the statistical distances and the extinction distance previously determined for Hu 1-2.

ACKNOWLEDGMENTS

We thank our anonymous referee for comments that have improved the presentation and discussion of the results. We are grateful to the group of support astronomers of the IAC for making us available the narrow-band filters used in the NOT observations. LFM, MB, and MAG acknowledge support by grant AYA2008-01934 of the Spanish MCINN (co-funded by FEDER funds). AR acknowledges support by grant AYA2008-06189-C03 of the Spanish MICINN (co-funded with FEDER funds). LFM acknowledges support from grant IN8458-2010/061 of Xunta de Galicia (co-funded by FEDER funds). The Digitized Sky Surveys were produced at the Space Telescope Science Institute under U.S.

Government grant NAG W-2166. The images of these surveys are based on photographic data obtained using the Oschin Schmidt Telescope on Palomar Mountain and the UK Schmidt Telescope. The plates were processed into the present compressed digital form with the permission of these institutions. The National Geographic Society - Palomar Observatory Sky Atlas (POSS-I) was made by the California Institute of Technology with grants from the National Geographic Society. The second Palomar Observatory Sky Atlas (POSS-II) was made by the California Institute of Technology with funds from the National Science Foundation, the National Geographic Society, the Sloan Foundation, the Samuel Oschin Foundation, and the Eastman Kodak Corporation. The Oschin Schmidt Telescope is operated by the California Institute of Technology and Palomar Observatory. The UK Schmidt Telescope was operated by the Royal Observatory Edinburgh, with funding from the UK Science and Engineering Research Council (later the UK Particle Physics and Astronomy Research Council), until 1988 June, and thereafter by the Anglo-Australian Observatory. Supplemental funding for sky-survey work at the STScI is provided by the European Southern Observatory.

REFERENCES

- Acker A., Marcout J., Ochsenbein F., Stenholm B., Tytenda R., 1992, Strasbourg-ESO Catalogue of Galactic Planetary Nebulae (Garching: ESO)
- Amnuel P.R., Guseinov O.Kh., Novruzova Kh.I., Rustamov Iu.S., 1984, A&SS, 107, 19
- Balick B., Rugers M., Terzian Y., Chengalur J.N., 1993, ApJ, 411, 778
- Balick B., Perinotto M., Maccioni A., Terzian Y., Hajian A., 1994, ApJ, 424, 800
- Borkowski K.J., Harrington J.P., 2001, ApJ, 550, 778
- Cahn J.H., 1976, AJ, 81, 407
- Fernández R., Monteiro H., Schwarz H., 2004, ApJ, 603, 595
- Frew D.J., 2008, Ph.D. Thesis, Macquarie University (Sydney)
- Guerrero M.A., Miranda L.F., 2011, A&A, submitted
- Guerrero M.A., Miranda L.F., Chu Y.-H., 2002, RMA&A (Conference Series), 12, 156
- Guerrero M.A., Miranda L.F., Manchado A., Vázquez R., 2000, MNRAS, 313, 1
- Hajian A.R., Terzian Y., 1996, PASP, 108, 258
- Liller W., 1965, PASP, 77, 25
- Manchado A., Guerrero M.A., Stanghellini L., Serra-Ricart M., 1996, *IAC Morphological Catalog of Northern Planetary Nebulae*, (IAC, La Laguna, Spain)
- Meaburn J., 1997, MNRAS, 292, L11
- Meaburn J., Lloyd M., Vaytet N.M.H., López J.A., 2008, MNRAS, 385, 269
- Miranda L.F., Blanco M., Guerrero M.A., Riera A., 2011, in *Planetary Nebulae: an eye to the future*, Proceedings IAU Symp.283 (Cambridge University Press), in press
- Miranda L.F., Torrelles J.M., Guerrero M.A., 1999, AJ, 117, 1421
- Miranda L.F., Torrelles J.M., Guerrero M.A., Vázquez R., Gómez Y., 2001, MNRAS, 321, 487
- Phillips S.R., 2004, MNRAS, 353, 589

- Phillips S.R., 2006, *RMA&A*, 42, 229
Pottasch S.R., 1983 in: *Planetary nebulae; Proceedings of the Symposium 103* (Dordrecht, Reidel), p. 391
Riera A., García-Lario P., Manchado A., Bobrowsky M., Estalella R., 2003, *A&A*, 401, 1039
Rodríguez L.F., Gómez Y., 2007, *RMA&A*, 43, 173
Sabaddin F., 1986, *A&AS*, 65, 301
Sabaddin F., Bianchini A, Hamzaoglu E., 1983, *A&AS*, 51, 119
Sabaddin F., Cappellaro E., Turatto M., 1987, *A&A*, 182, 305
Sahai R., Brillant S., Livio M., Grebel E.K., Brandner W., Tingay S, Nyman L.-A., 2002, *ApJ*, 573, L123
Sahai R., Trauger J.T., 1998, *AJ*, 116, 1357
Stanghellini L., Haywood M., 2010, *ApJ*, 714, 1096
Tafoya D., Imai H., Gómez Y., et al., 2011, *PASJ*, 63, 71